Title: **Supersonic Combustion Induced by Reflective Shuttling Shock Wave in Fan-Shaped Two-Dimensional Combustor**

Authors: MASATO YAMAGUCHI[1], KEN MATSUOKA[1], AKIRA KAWASAKI[1], JIRO KASAHARA[1], HIROAKI WATANABE[2], AKIKO MATSUO[2]

Affiliation 1: Department of Aerospace Engineering, Nagoya University
Furo-cho, Chikusa, Nagoya 464-8603, Aichi, Japan

Affiliation 2: Department of Mechanical Engineering, Keio University
3-14-1 Hiyoshi, Kouhoku-ku, Yokohama, Kanagawa 223-8522, Japan

Address: KEN MATSUOKA, Department of Aerospace Engineering, Nagoya University,
Furo-cho, Chikusa, Nagoya 464-8603, Japan
E-mail: matsuoka@nuae.nagoya-u.ac.jp
Fax: +81-52-789-3280

Colloquium: DETONATIONS, EXPLOSIONS, AND SUPERSONIC COMBUSTION including flame acceleration, DDT, and pulse-detonation, constant-volume combustion, and scramjet engines.

Total Length: 5503 Words
(Method: M1)

Main text:	2988 words
Equations:	92 words
Nomenclature:	274 words
References:	293 words
Figures:	1856 words

Abstract

As a novel detonation combustor that differs from a pulse and rotating detonation engine, a reflective shuttling detonation combustor (RSDC), in which detonation wave shuttles repeatedly, was proposed. In a fan-shaped two-dimensional combustor, detonation wave propagates, repeating attenuation and re-ignition by shock reflection at the side wall. In the demonstration experiment, chemiluminescence visualization and pressure measurement with ethylene–oxygen mixture were conducted at the same time. As the result, single shuttling wave coupled with pressure rise was observed in the combustor. The tangential velocity of the wave was 1526 ± 12 m/s and approximately 60 % of the estimated Chapman–Jouguet velocity of 2513 m/s. The ratio of pressure in front of the wave to one behind the primary wave or the reflected wave was in good agreement with one-dimensional shock theory, and it was suggested that the rapid reaction behind the reflected shock wave sustained the continuous propagation of the shock wave.

Keywords

Shock Induced Combustion, Reflected Shock Wave, Reflective Shuttling Detonation Combustor

Nomenclature

a	=	speed of sound
A_{inj}	=	total cross-sectional area of fuel or oxidizer injectors
D_{CJ}	=	Chapman–Jouguet (C–J) detonation speed
ER	=	equivalence ratio
L	=	arc length of combustor
$\dot{m}$	=	mass flow rate
p	=	absolute pressure
p_{ple}	=	absolute pressure of fuel or oxidizer in the plenums

r = distance from the origin of polar coordinate system

R = gas constant

t = time from spark ignition

T = temperature

v_t = tangential velocity of the wave

Greek symbols

Δp = pressure increase by the wave

Δt = time duration of one cycle of the wave

γ = specific heat ratio

θ = angle formed by the intersection of two lines

τ = time from the beginning of propagation

Subscripts

0 = value in front of shock wave

1 = value behind shock wave

2 = value behind reflected shock wave

am = ambient

ave = average

c = value for combustor

f = fuel

o = oxidizer

PT1 = value for pressure transducer installed at the side wall

PT2 = value for pressure transducer installed at the center of the combustor

st = value under stoichiometric conditions

1. Introduction

A detonation wave is a self-sustained combustion wave that propagates through detonable mixture at supersonic speed. Endo et al. [1] and Kindracki [2] confirmed that the thermal efficiency of the theoretical detonation cycle is higher than that of the isochoric cycle (Humphrey cycle) and isobaric cycle (Brayton cycle) in a conventional internal combustion engines. Moreover, because a detonation wave involves supersonic combustion, the burning process is completed instantaneously, and this makes it possible to reduce the scale of the combustor. A pulse detonation combustor (PDC) [3] has a cylindrical combustor, in which fuel is repeatedly burned by detonation waves. In a PDC, output power can be easily controlled owing to active detonation initiation by an ignition system and active supply of fuel and oxidizer by a valve mechanism. A pulse detonation cycle (PD cycle) also involves a cooling process in which low-pressure hot burned gas is purged by purging material, thereby making long-duration operating possible. Meanwhile, the thrust density is relatively small because of its intermittent combustion cycle. Therefore, the operation frequency must be raised to the gas-dynamic upper limit as determined by the combustor length [4]. Taki et al. [5] demonstrated a high-frequency PD cycle at an operation frequency of 1910 Hz by using a valveless oxidizer-supplying method and a piezo injector for fuel supply in a combustor with a length of 60 mm. However, to realize higher-frequency operation, the problems pertaining to shortening of the DDT process [6] and gas feeding at high speed must be overcome. A rotating detonation engine (RDE) is another type of detonation combustor, where one or more detonation waves continuously travel around an annular channel [7]. In contrast to a PDC, continuous propagation of detonation wave is realized in this combustor without a DDT process, while the gas dynamics in the combustor are insufficiently understood owing to its shape and curvature. Nakayama et al. [8] confirmed a detonation wave has a forward-tilting shape when a single detonation wave enters a two-dimensional combustor with curvature. Nakagami et al. [9] confirmed a forward-tilting detonation waves in an optically accessible disk-shaped combustor as well. Furthermore, Rankin et al. [10] also used an optically accessible

combustor whose outer wall was made of quartz to visualize fluid motion and OH* chemiluminescence in the combustor. Additionally, the RDE has problems with the thermal isolation of the inner cylinder and cooling against a high thermal load. As described above, each conventional detonation combustor has advantages and technical problems.

In this study, we propose a reflective shuttling detonation combustor (RSDC) that differs from a PDC and a RDE. Detonation wave propagates in a two-dimensional fan-shaped combustor, repeating attenuation and re-ignition by shock reflection at the side wall. Because of its two-dimensional thin geometry, it can be easily realized that continuous propagation of detonation wave, visualization of inner flow field, cooling of a wall of a combustor, and producing an arrayed system of combustors. In the present study, a stainless-steel two-dimensional fan-shaped combustor was produced by a metal 3D printer technique (Hakudo Inc.) and the combustor has a width of 5 mm and arc length L of 45 mm. Pressure measurement and chemiluminescence visualization were conducted at the same time by using gaseous ethylene as a fuel and gaseous oxygen as an oxidizer. As a result of the experiment, a single wave, which reciprocate repeatedly in the combustor at a velocity of v_t = 1526 ± 12 m/s, was observed. In this paper, the demonstration equipment of an RSDC, the experimental results and the propagating structure of the wave are described.

2. Experimental apparatus and conditions

2.1. Fan-shaped two-dimensional combustor

An image of the fan-shaped combustor (SUS630) made with a metal 3D printer and its schematic diagram are illustrated in Fig. 1. As shown in the front view of the combustor (middle of Fig. 1), a polar coordinate system (r, θ) was defined. The radius of the combustor's arc was r = 57.3 mm. The angle formed by the intersection of both sides of the combustor wall was θ = 45º. The arc length of the combustor was $L = r\theta$ = 45 mm. A pre-detonator with ethylene-oxygen mixture was applied to ignite and propagate a single detonation wave into the combustor. The coordinate at the center of the pre-detonator outlet was (r, θ) = (46.0 mm, 0º). For measurement of local pressure p_{PT1} at

the side wall (r, θ) = (54.4 mm, 3.0º) and p_{PT2} at the center of the combustor (r, θ) = (54.4 mm, 22.5º), high-frequency pressure transducers (PCB Piezotronics, lnc, 113B24) are installed flush with the combustor. The diameter of the pressure transducer was 5.54 mm and the limiting frequency was higher than 1MHz. Piezotronics pressure transducers (Keller 21Y series for plenums and Keller 23 series for the combustor) were applied to measure the static pressure p_f, p_o and p_c in the fuel and oxidizer plenums, and the combustor. The limiting frequencies were 2 kHz and 5 kHz, respectively. The value of p_c was measured at (r, θ) = (54.4 mm, 42.0º). The sampling rate of the pressure measurement was 5M points/s. Fifteen hole-shaped injectors for supplying detonable mixture were located at the arc of the combustor, and the center of each injector was at (r, θ) = (57.3 mm, 1.5 + 3iº) in the polar coordinate system, where i = 0 – 14. A cross-sectional view A-A of the combustor was shown at the right of Fig. 1. The width of the combustor and oxidizer plenum were both 5 mm. The oxidizer was supplied to the premixing room, whose diameter was 1.2 mm, and the combustor via a hole-shaped injector with a diameter of 0.9 mm. Likewise, fuel was supplied to the premixing room and the combustor through 0.5-mm-diameter hole-shaped injectors. The fuel and oxidizer met at right angles in the mixing room, and then the detonable mixture was supplied to the combustor. By placing the flat combustor shown in Fig. 1 between an acrylic plate and stainless steel plate, a two-dimensional fan-shaped combustor for chemiluminescence visualization was formed.

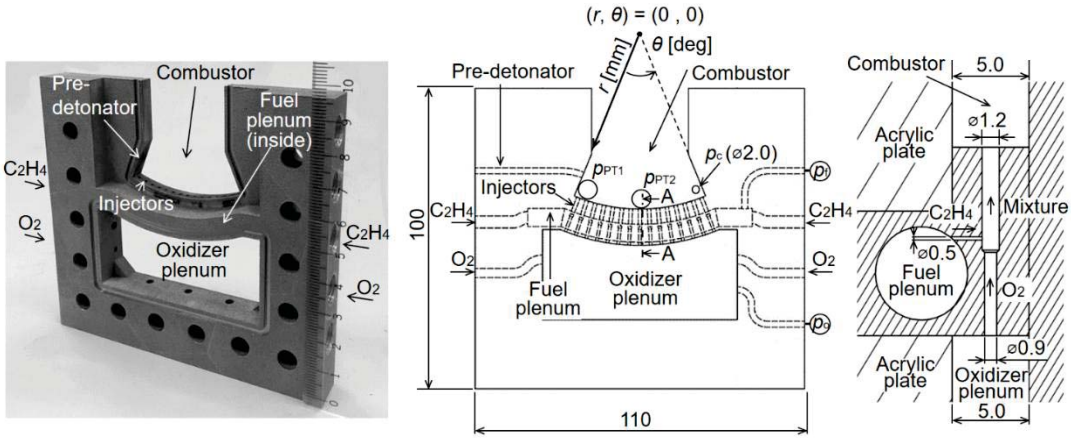

Fig. 1. Picture of 3D-printed combustor (left) (unit: cm), geometry of combustor (center), and cross-sectional view A-A (right) (unit: mm).

M1: (70 mm + 10 mm) × 2.2 words/mm × 2 columns + 20 words = 372 words

2.2. Experimental conditions

The time histories of the pressure p_f, p_o and p_c in the fuel and oxidizer plenums and combustor were given in Fig. 2. The time when the detonable mixture filled in the pre-detonator was ignited was defined as t = 0 s. The horizontal broken lines indicate the time-averaged pressure $p_{f,ave}$, $p_{o,ave}$ and $p_{c,ave}$ in the fuel and oxidizer plenums and the combustor in terms of t = 0 - 10 ms, and the values were $p_{f,ave}$ = 0.93 MPa, $p_{o,ave}$ = 0.66 MPa and $p_{c,ave}$ = 0.12 MPa, respectively. Ambient pressure and temperature was p_{am} = 0.10 MPa and T_{am} = 298 K, respectively.

As sown in Fig.1, the ratio of the pressure in the plenums to one in the combustor was sufficiently large. Therefore, it was assumed that the flow of ideal gas was choked at the injector, then, the mass flow rate $\dot{m}$ can be determined by using the following equation:

$$\dot{m} = \frac{p_{\mathrm{ple}} A_{\mathrm{inj}}}{\sqrt{R T_{\mathrm{ple}}}} \sqrt{\gamma \left(\frac{2}{\gamma + 1} \right)^{\frac{\gamma+1}{\gamma-1}}} \qquad (1)$$

where $p_{\mathrm{ple}}, T_{\mathrm{ple}}, A_{\mathrm{inj}}, R,$ and γ represent the total pressure in the plenum, total temperature in the plenum, cross-sectional area of the injector, gas constant and specific heat ratio, respectively. If the flow velocity upstream of the injector was relatively small and the static pressure was regarded as the total pressure, the mass flow rate of the fuel and oxidizer were estimated at $\dot{m}_f$ = 6.0 g/s, $\dot{m}_o$ = 15.6 g/s by using the following values: $p_{ple,f} = p_{f,ave}$ 0.93 MPa, $p_{ple,o} = p_{o,ave}$ = 0.66 MPa, $A_{inj,f}$ = 2.9 mm^2, $A_{inj,o}$ = 9.5 mm^2, γ_f = 1.24, γ_o = 1.40, R_f = 297 Jkg^{-1}K^{-1} and R_o = 260 Jkg^{-1}K^{-1}. Gas temperature T_{ple} in the high-pressure tank was assumed to be equivalent to ambient temperature T_{am}. An equivalence ratio can be estimated from the mass flow rate and the following equation:

$$ER = \frac{(\dot{m}_f/\dot{m}_o)}{(\dot{m}_f/\dot{m}_o)_{st}} \qquad (2)$$

where the subscript st denotes the detonable mixture under stoichiometric conditions. According to the estimated mass flow rate, the equivalence ratio of the detonable mixture was estimated at ER = 1.3.

A high-speed camera (Phantom, v2011), capable of capturing images at 341,463 frame/s (2.93 μs/frame) at 256 × 128 pixels and having an exposure time of 2.13 μs, was used to visualize inside the combustor. The surface imagery was 0.20 mm/pixel.

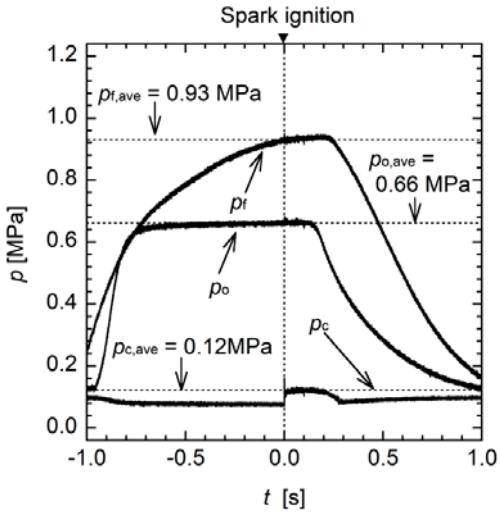

Fig. 2. Time histories of pressure p_f, p_o and p_c of fuel and oxidizer in plenums and combustor (p_{am} = 0.10 MPa, T_{am} = 298 K).

M1: (70 mm + 10 mm) × 2.2 words/mm × 1 column + 26 words = 202 words

3. Results and discussion

3.1 Time history of pressure in fan-shaped two-dimensional combustor

The time history of the pressure p_{PT1} and p_{PT2} acquired by the pressure transducer installed at (r, θ) = (54.4 mm, 3.0º) and (r, θ) = (54.4 mm, 22.5º) are shown in Fig. 3. The actual pressure waveform is shown at the left side of Fig. 3. The waveform gradually declines under the influence of the thermal load. Therefore, the pressure waveform was linearly approximated over a period of 5.0 ms ≤ t ≤ 5.5 ms by picking up every minimum value in one cycle. Then, the waveform was revised so that its time averaged minimum value $p_{PT1,min}$ and $p_{PT2,min}$ to be equal to $p_{c,ave}$ = 0.12 MPa. The revised figure was shown at the right side of Fig. 3. The symbols $p_{PT1,max}$ and $p_{PT2,max}$ in Fig.3 show averaged maximum value for

each cycle over a period of 5.0 ms ≤ t ≤ 5.5 ms. The error bar denotes a standard deviation over a period of 5.0 ms ≤ t ≤ 5.5 ms.

At first, a single detonation came from the pre-detonator reaching PT1 and PT2 at t = 1.3 ms, therefore, p_{PT1} and p_{PT2} increased rapidly. Immediately after the ignition, local explosion occurred at t = 2.3 ms. After t ≥ 2.8 ms, a cyclic pressure oscillation was recorded. As shown in Fig.3, the averaged pressure increase were Δp_{PT1} = 0.24 ± 0.01 MPa and Δp_{PT2} = 0.09 ± 0.01 MPa, respectively. The error bar denotes a standard deviation over a period of 5.0 ms ≤ t ≤ 5.5 ms. This suggests that a single wave repeatedly propagated and reflected in the combustor. This single propagation mode will be focused on in the following chapter.

A chemiluminescence visualization movie for 5.0 ms ≤ t ≤ 5.5 ms is shown in Fig. 4. The replay speed is 10 frame/s, which is about 30,000 times slower than the actual time scale. As can be seen in Fig. 4, chemical reactions were considered to be more active in high-brightness areas. Furthermore, higher-brightness areas were observed and propagate from side to side.

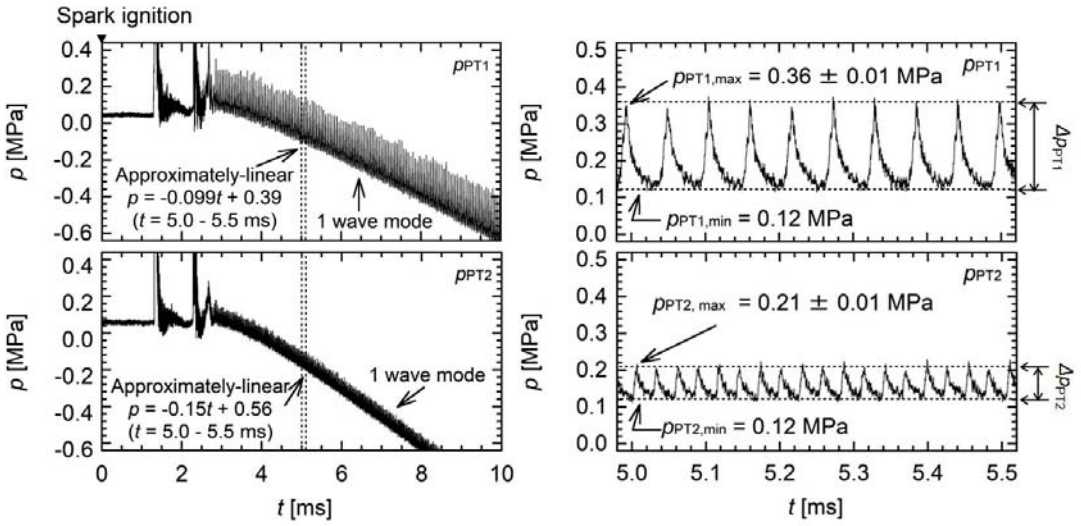

Fig. 3. Time history of pressure p_{PT1} and p_{PT2} in the combustor measured by pressure transducer installed at (r, θ) = (54.4 mm, 3.0º), (54.4 mm, 22.5º) (left), and corrected time history of pressure transducers (right).

M1: (70 mm + 10 mm) × 2.2 words/mm × 2 columns + 36 words = 388 words

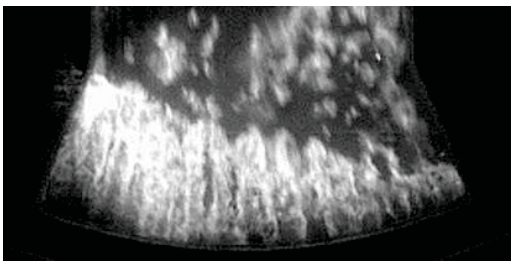

Fig. 4. Movie of the reciprocating wave (t = 5.0–5.5 ms).

M1: (34 mm + 10 mm) × 2.2 words/mm × 1 column + 12 words = 109 words

3.2 Tangential velocity of the wave

In this chapter, the time history of pressure p_{PT1} and p_{PT2} determined in the last chapter was compared with the chemiluminescence visualization movie to discuss the tangential propagation speed v_t and relation between the pressure and the wave. A time-corresponded figure of the time history of pressure p_{PT1} and p_{PT2} and the θ-t diagram at r = 54.4 mm for 5.0 ms ≤ t ≤ 5.5 ms was shown in Fig. 5. A tone reversal image was used for the θ-t diagram. Therefore, darker areas indicate higher-brightness areas in Fig. 4. A solid white line at θ = 3.0º and θ = 22.5º describes the center of the PT1 and PT2, respectively, and θ = 0º and 45.0º denote the bilateral side walls of the combustor. According to the black broken lines in Fig. 5, the pressure rise corresponded to the passing of the wave. At this point, the left wall θ = 0º was defined as the origin and the duration required by the wave to propagate one round trip as Δt. Then, the tangential velocity of the wave was obtained as a value of $v_t = 2r\theta/\Delta t$ = 1526 ± 12 m/s, where r = 54.4 mm and θ = 45 deg. The error bar indicates a standard deviation of nine cycles. If the upper sound speed was estimated to be a = 1190 m/s, the wave propagates at supersonic speed. The sound speed was calculated by using NASA-CEA online [11], assuming an adiabatic flame temperature at an average pressure of $p_{c,ave}$ = 0.12 MPa and ambient temperature T_{am} = 298 K. Consequently, it was suggested that the wave was accompanied by shock wave. However, the tangential velocity v_t was approximately 60% of the estimated C–J detonation velocity under the condition of ER = 1.3, $p_{c,ave}$ = 0.12 MPa and T_{am} = 298 K. This type of wave was also confirmed by Nakagami et al.[9] and its propagation velocity of v_t = 1600 m/s was close to the value which obtained in this study. The theoretical pressure at the C–J point represents 4.5 MPa under this

condition [11]. However, the experimental pressure was much lower than the ideal value. The pressure gains observed in the RDE so far were lower than the ideal value as well [12, 13]. The reason for lower propagation speed and less pressure increase will be discussed below.

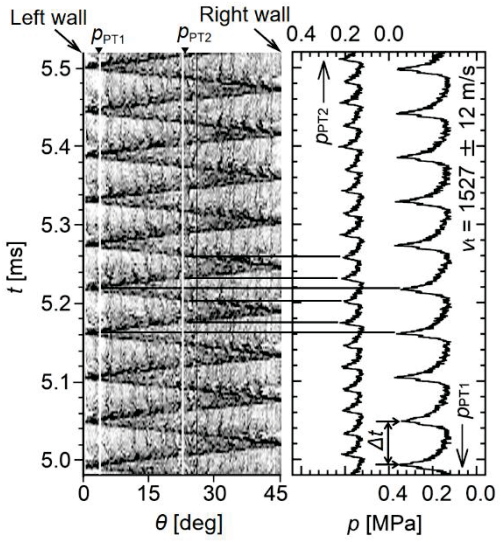

Fig. 5. θ–t diagram (r = 54.4 mm) with time history of pressure measured by pressure transducer installed at (r, θ) = (54.4 mm, 3.0º), (54.4 mm, 22.5º).

M1: (73 mm + 10 mm) × 2.2 words/mm × 1 column + 29 words =212 words

At the end of this chapter we deduce shock Mach number from p_{PT1} and p_{PT2}, which were obtained in chapter 3.1. As shown in Fig. 6, the conditions upstream of the normal shock wave, those behind the normal shock wave, and those behind the reflected shock wave are represented by subscripts 0, 1 and 2. Pressure ratios p_1/p_0 and p_2/p_0 can be acquired theoretically by assuming one-dimensional shock theory as following equations [14]:

$$\frac{p_1}{p_0} = 1 + \frac{2\gamma}{\gamma+1}(M_s^2 - 1) \qquad (3)$$

$$\frac{p_2}{p_0} = \frac{p_1}{p_0}\frac{\left(\frac{3\gamma-1}{\gamma-1}\right)\frac{p_1}{p_0} - 1}{\frac{p_1}{p_0} + \frac{\gamma+1}{\gamma-1}} \qquad (4)$$

where M_s indicate shock Mach number. In this study, we assume adiabatic flame for thermodynamic function, like γ

=1.12 and a = 1190 m/s [11]. Then, M_s = 1.30 can be obtained implicitly so as to the following value: $(p_1/p_0 - p_{PT2,max}/p_{PT2,min})^2 + (p_2/p_0 - p_{PT1,max}/p_{PT1,min})^2$, to be minimum. The pressure ratios were plotted in Fig.6 according to the deduced shock Mach number, and they were in good agreement with both theoretical lines within 2%. Furthermore, the shock Mach number was also in good agreement with the estimated value v_t/a = 1526/1190 = 1.28. Therefore, the propagating wave near the bottom of the combustor was correspond to one associate with a normal shock wave.

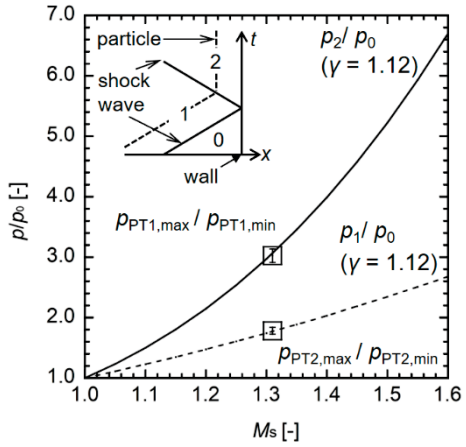

Fig. 6. The relation between shock Mach number and pressure ratios of p_1 to p_0 and p_2 to p_0.

M1: (60 mm + 10 mm) x 2.2 words/mm x 1 column + 19 words = 173 words

3.3 The Wave structure in one cycle

An enlarged view of Fig. 5 during 5.0 ms ≤ t ≤ 5.1 ms is shown at the left side of Fig.7, and the brightness value of chemiluminescence is shown for each time (a–j) at the right side of Fig. 6. The time τ = 0 μs in Fig. 6 is equal to t = 5.018 μs. The wall of the combustor and the position of the PT1 and PT2 are represented by white continuous line, and r = 54.4 mm is represented by black dashed line.

At the state (a), the shock wave reflected at the right wall began to propagate to the left at τ = 0 μs. At the state (b), the higher-brightness area propagated from right to left at τ = 5.86 μs. It could also be confirmed that a lower-brightness area at the bottom of the combustor in the state (a) and (b), where the chemical reaction was estimated to be inactive and the supplied detonable mixture from the injectors dominate this area. On the other hand, there was no area like this

immediately behind the higher-brightness area. This was because the chemical reaction was activated by higher temperature behind the shock wave. At the state (c), the front of the shock wave arrived at the edge of the PT2 and p_{PT2} began to rise at τ = 11.71 μs. Similarly, at the state (e), the front of the shock wave arrived at the edge of the PT1, and p_{PT1} began to rise at τ = 23.43 μs. According to the left side of Fig.7, p_{PT1} and p_{PT2} began to rise before the higher-brightness area came across the white lines. This is because the pressure transducer has a finite width. At the state (f), the shock wave started to propagate from left to right at τ = 29.29 μs after reflection at the right wall. In the vicinity of state (f), the waveform hit its peak right behind the reflected shock wave. A luminous intensity was higher behind the reflected shock wave. This was because the rapid reaction behind the reflected shock wave, which was due to higher temperature and increase in the area of the flame front by shock-flame interaction. Returning to state (c), (d) and (e), it can be clearly seen that the brightness decreases in the upper area after the reflected shock wave propagated. It is considered that the chemical reaction becomes inactive, and finally, the brightness is lower than what the high-speed camera can detect. The same phenomenon was also observed at the time of state (h), (i) and (j). In consequent, there is a possibility that the rapid reaction behind the reflected shock wave sustains the shock wave not to be attenuated.

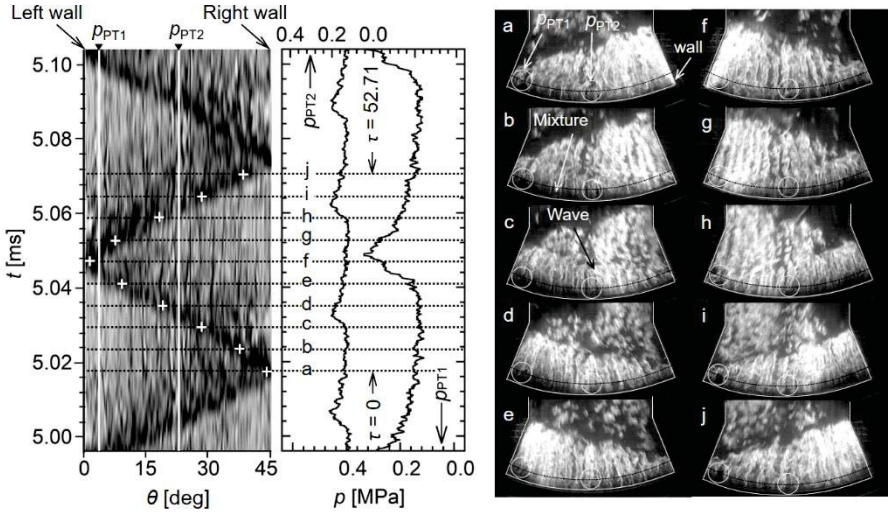

Fig. 7. Enlarged view of θ–t diagram (r = 54.4 mm) with time history of pressure measured by pressure transducer installed at (r, θ) = (54.4 mm, 3.0º), (r, θ) = (54.4 mm, 22.5º) (left) and single-cycle images (t = 5.0–5.1 ms) of the shock wave.

M1: (70 mm + 10 mm) × 2.2 words/mm × 2 column + 48 words = 400 words

4. Conclusions

In this study, we proposed new detonation combustor, Reflective Shuttling Detonation Combustor. Pressure measurement and chemiluminescence visualization were conducted at the same time by using gaseous ethylene as a fuel and gaseous oxygen as an oxidizer. As a results, it was confirmed that a single wave propagates stably by repeating the reflection at the side wall of the combustor. This wave was accompanied by a rapid increase in the pressure. Therefore, it was considered to be coupled with the shock wave. However, the tangential velocity of this wave was $v_t = 1526 \pm 12$ m/s, and the value was smaller than the estimated C–J detonation value by 40%. This was because the wave corresponds to one associated with normal shock wave. Moreover, it is suggested that the reason why shock wave can propagate without attenuation was due to rapid combustion near the side wall behind the reflected shock wave.

The phenomenon, which combustion is induced by reflected shock wave, probably has advantages such as the enhancement of mixing and/or combustion by using shock wave. Moreover, it is expected that the combustor is applied to engines for small spacecraft and large ramjet engines [15] without inner cylinders.

Acknowledgements

This work was subsidized by a Grand-Aid for scientific research (A) (No. 17H04971) and Tatematsu Foundation.

References

[1] Endo, T., Yatsufusa, T., Taki, S., and Kasahara, J., Science and Technology of Energetic Materials, 65 (103) (2004) 103–110 [in Japanese].

[2] J. Kindracki, Badania eksperymentalne i symulacje numeryczne procesu inicjacji wirują˛cej detonacji gazowej, Ph.D. thesis (in Polish), Politechnika Warszawska, Warsaw, Poland, 2008.

[3] J.A. Nicholls, H.R. Wilkinson, R.B. Morrison, Jet Propul. 27 (5) (1957) 534–541.

[4] H. Watanabe, A. Matsuo, K. Matsuoka, J. Kasahara, 55th AIAA Aerospace Sciences Meeting (2017) 1284-1295.

[5] T. Haruna, N. Hirota, K. Matsuoka, A. Kawasaki, J. Kasaahra, H. Watanabe, A. Matsuo, T. Endo, 26th international colloquium on the dynamics of explosions and reactive systems, Boston, MA (2017).

[6] O.Peraldi, R. Knystautas, J.H. Lee.Proc. Combust. 21 (1986)1629-1637

[7] F.A. Bykovskii, S.A. Zhdan, E. F. Vedemikov, J.Propul Power, 22 (6) (2006) 1204-1216

[8] H. Nakayama, J. Kasahara, A. Matsuo, I Funaki, Proc. Combust. 34 (2) (2013) 1939-1947

[9] S. Nakagami, K. Matsuoka, J. Kasahara, A. Matsuo, I. Funaki, Proc. Combust. 36 (2017) 2673–2680

[10] B. A. Rankin, D. R. Richardson, A. W. Caswell, A. G. Naples, J. L. Hoke, F. R. Schauer, Combustion and Flame 176 (2017) 12–22

[11] S. Gordon, B.J. McBride, NASA SP-273, online version available at https://www.grc.nasa.gov/WWW/CEAWeb/, 1971.

[12] J. Kindracki, P. Wolański, Z. Gut, Shock Waves 21 (2011) 75–84

[13] Y. Liu, Y. Wang, Yongsheng. Li, Yang. Li, J. Wang, Chinese Journal of Aeronautics 28 (3) (2015) 669–675

[14] L.D. Landau, E.M. Lifshitz, Fluid Mechanics 2nd edition, Butterworth- Heinemann, Oxford, UK, 1987, p.335, 378

[15] P. Wolański, Journal of KONES Powertrain and Transport 18 (3) (2011) 515–521

Table and figure captions

Fig. 1. Picture of 3D-printed combustor (left) (unit: cm), geometry of combustor (center), and cross-sectional view A-A (right) (unit: mm).

Fig. 2. Time histories of pressure p_f, p_o and p_c of fuel and oxidizer in plenums and combustor (p_{am} = 0.10 MPa, T_{am} = 298 K).

Fig. 3. Time history of pressure p_{PT1} and p_{PT2} in the combustor measured by pressure transducer installed at (r, θ) = (54.4 mm, 3.0º), (54.4 mm, 22.5º) (left), and corrected time history of pressure transducers (right).

Fig. 4. Movie of the reciprocating wave (t = 5.0–5.5 ms).

Fig. 5. θ–t diagram (r = 54.4 mm) with time history of pressure measured by pressure transducer installed at (r, θ) = (54.4 mm, 3.0º), (54.4 mm, 22.5º).

Fig. 6. The relation between shock Mach number and pressure ratios of p_1 to p_0 and p_2 to p_0.

Fig. 7. Enlarged view of θ–t diagram (r = 54.4 mm) with time history of pressure measured by pressure transducer installed at (r, θ) = (54.4 mm, 3.0º), (r, θ) = (54.4 mm, 22.5º) (left) and single-cycle images (t = 5.0–5.1 ms) of the shock wave.